



Effect of Sintering Temperature on Structural and Dielectric Properties of $\text{Li}_{0.30}\text{Cr}_{0.02}\text{Ni}_{0.68}\text{O}$ Ceramic Doped With Kaolinite

Metha Rattanapithaksuk* Jinda Khemprasit^{†, **}

(Received: May 19, 2020; Revised: August 14, 2020; Accepted: August 20, 2020)

ABSTRACT

$\text{Li}_{0.30}\text{Cr}_{0.02}\text{Ni}_{0.68}\text{O}$ (LCNO) ceramics were prepared by sol-gel process and then doped with 1 %wt. kaolinite via solid state reaction. All doped samples were sintered at 1100-1300 °C. All sintered samples showed the single phase of cubic rock-salt NiO structure without extra phases. The microstructure of LCNO exhibited polyhedral grains with grain size of ~10-50 μm . With doping 1 %wt. kaolinite, the grain sizes were decreased to 0.5-5 μm . The grain sizes were increased with an increase of sintering temperatures. The grains were denser and larger as sintering temperature increased to 1300 °C. The dielectric properties of the 1% wt. kaolinite-doped LCNO ceramic were the highest dielectric constant (3.40×10^5) at 10 kHz and room temperature. Its loss tangent was 2.44 which was 2 times lower than that of the pure LCNO. The high dielectric constants can be explained by BLCs model.

Keywords: $\text{Li}_{0.30}\text{Cr}_{0.02}\text{Ni}_{0.68}\text{O}$, Kaolinite, Dielectric properties

[†]Corresponding author: jinda@kku.ac.th

*Student, Master of Science (Chemistry), Department of Chemistry, Faculty of Science, Khon Kaen University, Thailand

**Assistant Professor, Department of Chemistry, Faculty of Science, Khon Kaen University, Thailand



Introduction

Lead-free and non-ferroelectric materials with giant dielectric constant values ($\epsilon_r \sim 10^4$ - 10^5) have been found in $\text{CaCu}_3\text{Ti}_4\text{O}_{12}$ (CCTO) [1-3] and (A,B)- doped NiO ceramics (where A = Li, Na, K ions and B = Ti, Cr, Al, V, Fe, Co, W, Pr, Zr, La ions) [4-12] for applications as capacitors and memory devices. The dielectric constants of these giant dielectric materials are also weakly dependent on temperature and frequency. The giant dielectric response in these materials is explained by the boundary layer capacitor (BLC) structures, corresponding to an electrically heterogeneous structure which consists of semiconducting grains and insulating grain boundaries [13]. However, loss tangents ($\tan\delta$) of these materials are very high, not suitable for capacitor applications. The reduction of $\tan\delta$ by adding the high-electrical resistivity dopants into dielectric materials has been studied such as MgO [13-14], ZrO_2 [15], CaTiO_3 [16] and SiO_2 [17] into CCTO, SiO_2 into $(\text{Ba},\text{Sr})\text{TiO}_3$ [18], Al_2O_3 into $\text{Li}_x\text{Cr}_y\text{Ni}_{1-x-y}\text{O}$ [5] and kaolinite into BaTiO_3 [19] in order to increase the electrical resistivity at grain boundary. For instance, Sun and coworkers [13] have studied the dielectric response in Mg-doped CCTO ceramics and found that the dielectric constant of the Mg (x=0.05) doped CCTO ($\epsilon_r \sim 5.32 \times 10^4$) was a little higher than that of the pure CCTO ($\epsilon_r \sim 2.00 \times 10^4$), relating to uniform microstructure with large grains of the doped CCTO. In addition, the loss tangent of the doped CCTO ($\tan\delta=0.017$) was lower than that of the pure CCTO ($\tan\delta=0.041$). Tang and coworkers have reported that the loss tangent decreased when SiO_2 was added into CCTO nanowires [17]. The loss tangent of the 40 % SiO_2 /CCTO nanowires is 0.081, which is lower than that of the CCTO nanowires ($\tan\delta=0.35$). Khumpaitool and coworkers have synthesized Al_2O_3 -doped $\text{Li}_{0.30}\text{Cr}_{0.02}\text{Ni}_{0.68}\text{O}$ (LCNO) by solid-state reaction via sol-gel process [5]. The 0.2 wt.% Al_2O_3 /LCNO has the highest ϵ_r value (7.25×10^6) and the lowest $\tan\delta$ (2.37) at 1 kHz with stability of $\tan\delta$ over the measured frequency, which are better than those of the pure LCNO ($\epsilon_r = 4.42 \times 10^5$; $\tan\delta = 15.80$). It is found that the $\tan\delta$ of the Al_2O_3 -doped sample is nearly 7 times lower than that of the pure LCNO sample. Chen and coworkers have prepared BaTiO_3 /kaolinite composites by conventional solid-state method [19]. XRD results showed that the new phase $\text{BaAl}_2\text{Si}_2\text{O}_8$ was formed as kaolinite added into BaTiO_3 and effect to decrease the $\tan\delta$.

Objectives of the study

In this work, $\text{Li}_{0.30}\text{Cr}_{0.02}\text{Ni}_{0.68}\text{O}$ (LCNO) was prepared by sol-gel process and improvement of $\tan\delta$ of this material by adding the high-electrical resistivity dopant was considered. Kaolinite is clay that much interest because of its high electrical resistivity (1×10^3 - $2.22 \times 10^4 \Omega \cdot \text{cm}$) and low cost. Therefore, kaolinite was chosen to dope into LCNO in order to reduce $\tan\delta$ while keeping high dielectric constant. Moreover, the effect of sintering temperature on structural and dielectric properties of kaolinite/ $\text{Li}_{0.30}\text{Cr}_{0.02}\text{Ni}_{0.68}\text{O}$ composite ceramics was also investigated.

Methodology

Research methodology of this study consists of three parts including the preparation of LCNO, the preparation of kaolinite-doped LCNO and characterization.

Preparation of LCNO

LiNO_3 , $\text{Cr}(\text{NO}_3)_3 \cdot 9\text{H}_2\text{O}$ and $\text{Ni}(\text{NO}_3)_2 \cdot 6\text{H}_2\text{O}$ were used as starting materials and ethylene glycol was used as cross linking agent. LiNO_3 and $\text{Ni}(\text{NO}_3)_2 \cdot 6\text{H}_2\text{O}$ were dissolved in deionized water to get a clear solution. $\text{Cr}(\text{NO}_3)_3 \cdot 9\text{H}_2\text{O}$ in stoichiometric proportion was then slowly added into the solution and refluxed for 2 h, followed by heating on a hot plate at 250 °C to get dried gel. The dried gel was calcined at 1000 °C for 3 h and then sintered at 1300 °C for 3 h to get oxide powder.

Preparation of kaolinite-doped LCNO

The LCNO sintered powder was ground and sieved using a 200 mesh sieve. The 1 wt% kaolinite powder was mixed with LCNO powder by using ZrO_2 ball milling for 6 h. The kaolinite-doped LCNO material was mixed with 3% Polyvinyl alcohol (PVA) as a binder and pressed into pellets of 11 mm in diameter and ~1-2 mm in thickness by hydraulic pressing method at 5 tons. The sintering temperatures for making kaolinite-doped LCNO materials were 1100, 1200 and 1300 °C. The products were sintered for 2 h in a muffle furnace with a heating rate of 5 °C/min, and then coated with silver electrode.

Characterization

Phase composition of the sintered pellet samples was identified using an X-ray diffractometer (XRD, PANalytical, Empyrean) with $\text{Cu K}\alpha$ radiation, a scan step of 0.02 from 10° to 80° (2θ). Microstructure of the sintered pellet samples was observed using scanning electron microscopy (SEM, LEO-1450VP). Capacitance and $\tan\delta$ measurements were performed using an impedance analyzer (HP4194A, Agilent) at frequency range from 100 Hz to 1 MHz and temperature range from -60 to 200 °C.

Results and discussions

The XRD patterns of kaolinite-doped LCNO samples sintered at various temperatures are shown in Figure 1. All sintered samples show the single phase of cubic rock salt structures [JCPDS No. 47-1049] without extra phase, consistent with other works [5-6, 8]. When sintering temperature was increased from 1100 to 1200 °C, the peak intensity slightly increased due to the increase of crystallinity that is related to the increase of crystallite size. The crystallite size was calculated by the Scherrer equation using the full-width at half maximum height (FWHM) of three diffraction peaks as (111), (200) and (220). The crystallite size increases rapidly from 91 nm to 138 nm when the sintering temperature is changed from 1100 °C to 1200 °C. The lattice parameters are slightly changed with increasing sintering temperatures. That can be implied that no interdiffusion between LCNO and kaolinite phases occurs even at higher sintering temperature. Furthermore, the relative densities increase from 44.76% for the sample sintered at 1100 °C to 56.64% for the sample sintered at higher sintering temperature. The crystallite size, lattice parameter, relative density and grain size of all sintered samples are summarized in Table 1.

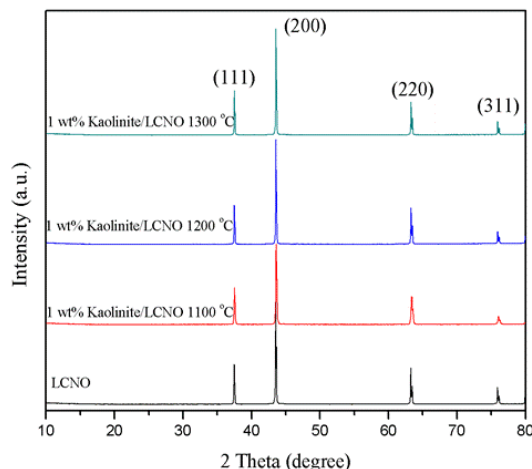


Figure 1 XRD patterns of the pure LCNO and kaolinite-doped LCNO samples sintered at various temperatures

Table 1 Summary of lattice parameter, crystallite size, relative density, grain size and dielectric properties of the pure LCNO and kaolinite-doped LCNO samples sintered at various temperatures

Samples	Lattice parameter a (Å)	Crystallite size ^a (nm)	Relative density ^b (%)	Grain size (μm)	ϵ_r at 10 kHz	$\tan\delta$ at 10 kHz
LCNO	3.318	91.5	56.58	10-50	3.13×10^4	4.14
1wt.% Kaolinite/LCNO-1100	3.319	91.0	44.76	0.5-5	3.40×10^5	2.44
1wt.% Kaolinite/LCNO-1200	3.320	138.0	53.52	1-5	1.22×10^4	1.42
1wt.% Kaolinite/LCNO-1300	3.319	138.0	56.64	5-20	1.11×10^4	1.48

a Calculated by Scherrer equation

b Determined by using Archimedes method

Figure 2 shows the SEM images of surfaces (left hand images) and fracture surfaces (right hand images) of pure LCNO and kaolinite-doped LCNO with various sintering temperatures (1100 °C, 1200 °C and 1300 °C). The pure LCNO reveals polyhedral grains with grain sizes of 10 to 50 μm. With 1 wt% kaolinite doping, uniformly small spherical grains appear (grain sizes ~ 0.5 to 5 μm). After that, as the sintering temperature is increased, the grain sizes increase, because of the agglomeration of small grains at higher sintering temperature. Grain size decreases with kaolinite doping because kaolinite particles could prevent the ion diffusion of LCNO phase and inhibit the grain growth of LCNO, corresponding with other work [18].

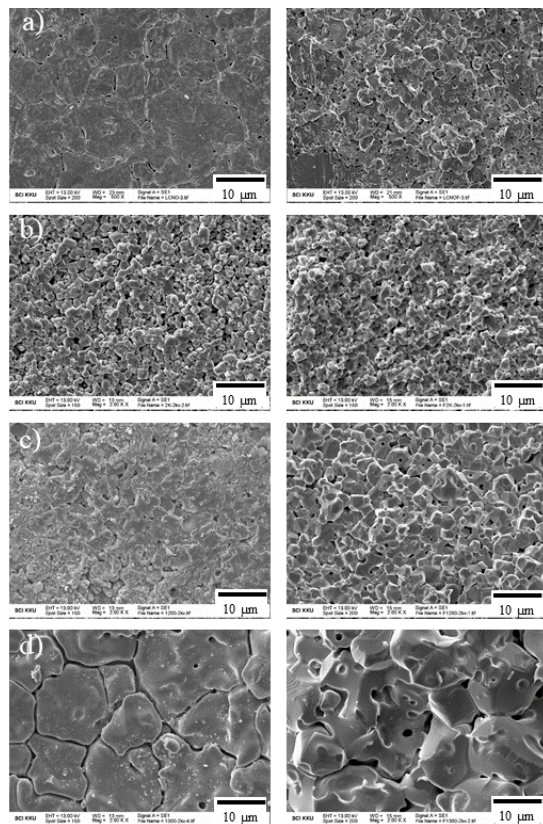


Figure 2 SEM images of surfaces (left hand images) and fracture surfaces (right hand images) of (a) the pure LCNO and the kaolinite-doped LCNO samples sintered at (b) 1100 °C (c) 1200 °C and (d) 1300 °C

The dielectric properties (ϵ_r and $\tan\delta$) of kaolinite-doped LCNO with various sintering temperatures as a function of frequency are shown in Figure 3. It was found that all samples show very high dielectric constants ($\sim 10^4$ - 10^7). However, higher dielectric constants which are found at low frequency are observed for all samples, especially for the doped sample sintered at 1100 °C. That is due to the space charge polarization which occurs at low frequency, as also reported in other works [2, 5-6]. The sample sintered at 1100 °C exhibits the highest dielectric constant ($\epsilon_r \sim 10^5$ - 10^7), relating to smaller spherical grains with more uniform and more dense grains when compared to others. The other sintering temperatures were agglomeration of small grains which ϵ_r is lower than sample sintered at 1100 °C. For loss tangent, the doped sample sintered at 1100 °C has the low loss tangent, which is rather stable over the measured frequency range, relating to the smaller, denser and more uniform grains when compared to the pure LCNO and other sintering temperatures. However, its $\tan\delta$ is a little higher than those of other doped samples. The dielectric properties measured at room temperature and various frequencies are summarized in Table 1.

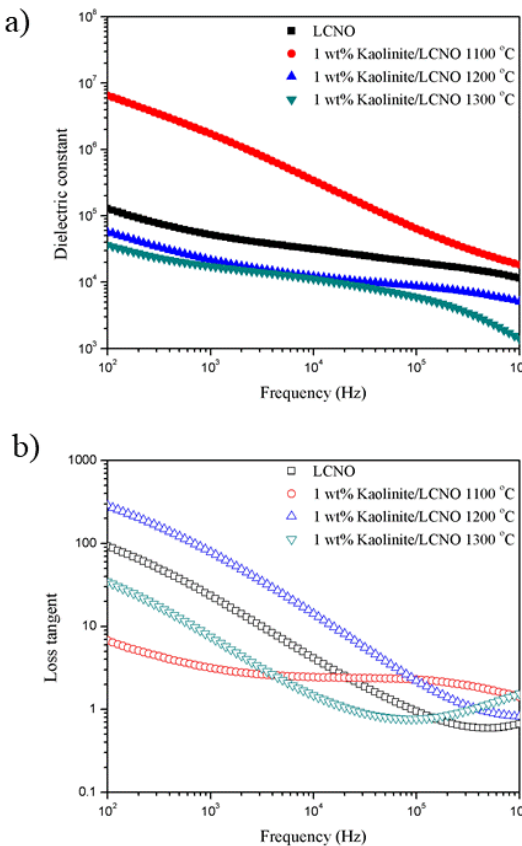


Figure 3 Frequency dependence of (a) dielectric constant and (b) loss tangent measured at room temperature of the pure LCNO and kaolinite-doped LCNO samples with various sintering temperatures

Figure 4 presents the temperature dependence of dielectric properties of kaolinite-doped LCNO with various sintering temperatures from 1100 to 1300 °C. The ϵ_r of all samples, except the doped LCNO sintered at 1100 °C, increase gradually with increasing temperature. Whereas, the weakly temperature dependent peak with the peak at ~70 °C is observed for the doped samples sintered at 1100 °C, which is in agreement with other reports [20-21]. Y. Pu et al. [21] reported that dielectric constant of the kaolinite-doped $\text{CaCu}_3\text{Ti}_4\text{O}_{12}$ (CCTO) was lower than that of the pure CCTO and the phase transition peak temperatures shifted to higher values with an increase of the kaolinite content. The loss tangents of doped samples, except the doped LCNO sintered at 1100 °C, are nearly constant over temperature range from -60 °C to 120 °C and then increase with increasing temperature above 120 °C, that is due to charge mobility at high temperature. The sample sintered at 1100 °C exhibits the strong temperature dependence of the loss tangent with the peak at ~70 °C, that could be implied the phase transition. The best dielectric properties are found for the doped sample sintered at 1100 °C, its dielectric constant and loss tangent at 10 kHz, and room temperature are 3.40×10^5 and 2.44, respectively, which are better than those of the pure LCNO ($\epsilon_r = 3.13 \times 10^4$, $\tan\delta = 4.14$ at 10 kHz). It is noted that kaolinite doping into LCNO can reduce the $\tan\delta$ by 2 times.

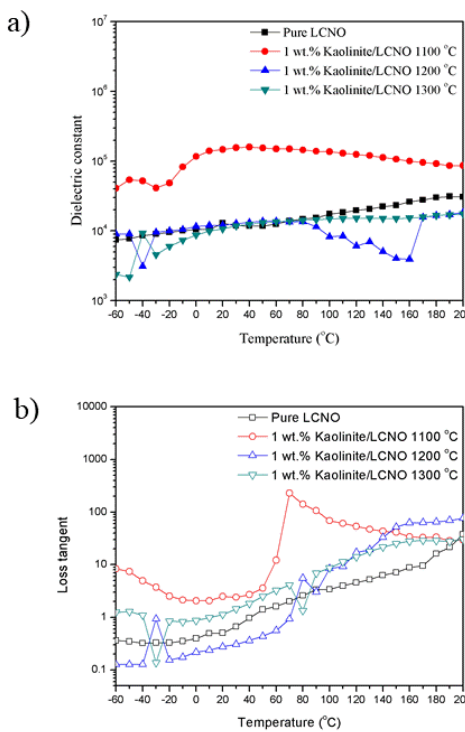


Figure 4 Temperature dependence of (a) dielectric constant and (b) loss tangent measured at 10 kHz of the pure LCNO and kaolinite-doped LCNO samples with various sintering temperatures

The Cole-Cole plots of pure LCNO and kaolinite-doped LCNO with various sintering temperatures are shown in Figure 5. The results indicate that the kaolinite doping and the increased sintering temperature cause the increase of electrical resistance at grain boundaries that could be observed from the magnitude of each semicircle on Z' axis. The large semicircular arcs show non-zero intercept as shown in the inset of Figure 5. Therefore, the electrical response is attributed to heterogeneous structure consisting of semiconducting grain of LCNO ceramic corresponding to other research [22]. J. Khemprasit et al. displayed the complex impedance spectroscopy of Cr-doped LCNO and found that a large semicircular arc with a non-zero intercept on the Z' axis at high frequency represented the contribution of semiconducting grains, while the low frequency arc represented the contribution of insulating grain boundaries.

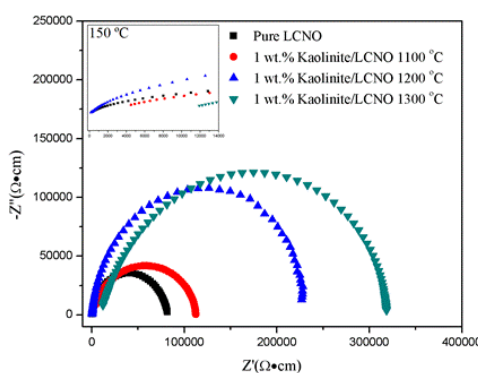


Figure 5 Complex impedance of the pure LCNO and kaolinite-doped LCNO samples with various sintering temperatures

Conclusions

The $\text{Li}_{0.30}\text{Cr}_{0.02}\text{Ni}_{0.68}\text{O}$ ceramics doped with kaolinite were successfully synthesized by solid state reaction via sol-gel process. All samples exhibited the single phase of the cubic rock-salt NiO structure without extra phase. The grain size of doped LCNO was smaller than that of the pure LCNO however when the sintering temperature was increased the grain size increased. All doped LCNO samples showed very high dielectric constants. The highest ϵ_r (3.40×10^5) and the low $\tan\delta$ (2.44) at 10 kHz and room temperature were observed for the doped LCNO sintered at 1300 °C that its $\tan\delta$ is lower than the pure LCNO ($\tan\delta = 4.14$).

Acknowledgements

This work was financially supported by the Center of Excellence for Innovation in Chemistry (PERCH-CIC), the Materials Chemistry Research Center (MCRC), Department of Chemistry, Faculty of Science, Khon Kaen University, for providing use of their instruments facility.

References

1. Liu P, Lai Y, Zeng Y, Wu S, Huang Z, Han J. Influence of sintering conditions on microstructure and electrical properties of $\text{CaCu}_3\text{Ti}_4\text{O}_{12}$ (CCTO) ceramics. *J Alloy Compd.* 2015; 650: 59-64.
2. Schmidt R, Stennett MC, Hyatt NC, Pokorny J, Prado-Gonjal J and Li M. Effects of sintering temperature on the internal barrier layer capacitor (IBLC) structure in $\text{CaCu}_3\text{Ti}_4\text{O}_{12}$ (CCTO) ceramics. *J Eur Ceram Soc.* 2012; 32: 3313-3323.
3. Mazumder R, Seal A, Sen A, Maiti HS. Effect of Boron Addition on the Dielectric Properties of Giant Dielectric $\text{CaCu}_3\text{Ti}_4\text{O}_{12}$. *Ferroelectrics.* 2005; 326: 103-108.
4. Maensiri S, Thongbai P, Yamwong T. Giant dielectric permittivity observed in $\text{CaCu}_3\text{Ti}_4\text{O}_{12}/(\text{Li},\text{Ti})$ -doped NiO composites. *Appl Phys Lett.* 2007; 90: 202908.
5. Khumpaitool B, Khemprasit J. Improvement in dielectric properties of Al_2O_3 -doped $\text{Li}_{0.30}\text{Cr}_{0.02}\text{Ni}_{0.68}\text{O}$ ceramics. *Mat Lett.* 2011; 65: 1053–1056.
6. Tangwancharoen S, Thongbai P, Yamwong T, Maensiri S. Dielectric and electrical properties of giant dielectric (Li, Al)-doped NiO ceramics. *Mat Chem Phys.* 2009; 115: 585–589.
7. Chen GJ, Hsiao YJ, Chang YS, Chai YL. Structure and high dielectric permittivity of $\text{Li}_{0.01}\text{M}_{0.05}\text{Ni}_{0.94}\text{O}$ (M=V and W) ceramics. *J Alloy Compd.* 2009; 474: 237-240.
8. Thongbai P, Yamwong T, Maensiri S. Effects of Li and Fe doping on dielectric relaxation behavior in (Li, Fe)-doped NiO ceramics. *Mat Chem Phys.* 2010; 123: 56–61.
9. Li Y, Fang L, Liu L, Huang Y, Hu C. Giant dielectric response and charge compensation of Li- and Co-doped NiO ceramics. *Mat Sci Eng B.* 2012; 177: 673–677.

10. Dakhel AA. (Giant dielectric permittivity in Li and Pr co-doped NiO ceramics. *J Alloy Compd.* 2009; 488: 31-34.
11. Manna S, De SK. Giant dielectric permittivity observed in Li and Zr co-doped NiO. *Solid State Commun.* 2010; 150: 399-404.
12. Dakhel AA. Dielectric relaxation behavior of Li and La co-doped NiO ceramics. *Ceram Int.* 2013; 39: 4263-4268.
13. Sun L, Zhang R, Wang Z, Cao E, Zhang Y, Ju L. Microstructure and enhanced dielectric response in Mg doped $\text{CaCu}_3\text{Ti}_4\text{O}_{12}$ ceramics. *J Alloy Compd.* 2016; 663: 345-350.
14. Thongbai P, Yamwong T, Maensiri S. Non-Ohmic and dielectric properties of $\text{CaCu}_3\text{Ti}_4\text{O}_{12}$ -MgO nanocomposites. *Microelectron Eng.* 2013; 108: 177-181.
15. Espinoza-González R, Mosquera E. Influence of micro- and nanoparticles of zirconium oxides on the dielectric properties of $\text{CaCu}_3\text{Ti}_4\text{O}_{12}$. *Ceram Int.* 43: 2017; 14659-14665.
16. Yan Y, Jin L, Feng L, Cao G. Decrease of dielectric loss in giant dielectric constant $\text{CaCu}_3\text{Ti}_4\text{O}_{12}$ ceramics by adding CaTiO_3 . *Mat Sci Eng B.* 2006; 130: 146-150.
17. Tang H, Zhou Z, Bowland CC, Sodano HA. Synthesis of calcium copper titanate ($\text{CaCu}_3\text{Ti}_4\text{O}_{12}$) nanowires with insulating SiO_2 barrier for low loss high dielectric constant nanocomposites. *Nano Energy.* 2015; 17: 302-307.
18. Diao C, Liu H, Hao H, Cao M, Yao Z. Effect of SiO_2 additive on dielectric response and energy storage performance of $\text{Ba}_{0.4}\text{Sr}_{0.6}\text{TiO}_3$ ceramics. *Ceram Int.* 2016; 42: 12639-12643.
19. Chen K, Pu YP, Liu JK. Crystal structure and dielectric properties of barium titanate-kaolinite composites. *Ceram Int.* 2012; 38S: S101-S104.
20. Pu Y, Chen K, Wu H. Effects of kaolinite addition on the densification and dielectric properties of BaTiO_3 ceramics. *J Alloy Compd.* 2011; 509: 8561-8566.
21. Pu Y, Hu Y, Wang P, Sun Z, Liu X, Dong Z. Effect of kaolinite-doping on the microstructure and the dielectric properties of $\text{CaCu}_3\text{Ti}_4\text{O}_{12}$ ceramics. *Ceram Int.* 2015; 41: S818-S822.
22. Khemprasit J, Khumpaitool B. Influence of Cr doping on structure and dielectric properties of $\text{Li}_x\text{Cr}_y\text{Ni}_{1-x-y}\text{O}$ ceramics. *Ceram Int.* 2015; 41: 663-669.